4 Optical Coherence Tomography Angiography in Macular Disorders

Colin S. Tan, Louis W. Lim, and Srini Vas R. Sadda

4.1 Introduction

Advances in ocular imaging technology, particularly imaging of the retina and choroid, have revolutionized the practice of ophthalmology in recent years. In addition to color fundus photos and fluorescein and indocyanine green angiography [1–3], newer imaging modalities such as optical coherence tomography (OCT), widefield imaging [4–7] and multicolor imaging have assumed increasingly important roles in the diagnosis, monitoring, and management of various retinal diseases. Optical coherence tomography angiography (OCTA) is a novel and exciting technology that has revolutionized the practice of ophthalmology in the few years since its introduction in commercial imaging devices. This chapter describes OCTA technology, discusses its applications among common retinal conditions, and reviews its strengths and limitations.

C. S. Tan (✉)
National Healthcare Group Eye Institute, Tan Tock Seng Hospital, Singapore, Singapore

Fundus Image Reading Center, National Healthcare Group Eye Institute, Singapore, Singapore

Duke-NUS Medical School, Singapore, Singapore

Lee Kong Chian School of Medicine, Nanyang Technological University, Singapore, Singapore

L. W. Lim
National Healthcare Group Eye Institute, Tan Tock Seng Hospital, Singapore, Singapore

S. V. R. Sadda
Doheny Eye Institute, University of California Los Angeles, Los Angeles, CA, USA
e-mail: ssadda@doheny.org

4.2 Principles of OCTA

OCTA is a noninvasive imaging modality that utilizes OCT technology to produce en face images of the retinal, subretinal, and choroidal vasculature (Figs. 4.1, 4.2, and 4.3).

Due to the improvements in scanning speed, OCTA devices are able to rapidly acquire repeated B-scans at the same location of the eye. Variations between B-scans are the result of moving objects such as blood flow, while stationary objects will appear similar at different time points. Thus, these repeated B-scans allow for blood flow to be detected in the form of changes in signal amplitude and/or phase. Repeated B-scan images at a particular retinal location are compared to each other using algorithms to generate a motion contrast image. Volumetric data of the retina are then produced by repeating these B-scans at different locations on the retina—typically in a raster scan pattern. The volumetric data produced can be segmented at different layers of the retina and choroid, thereby producing vascular flow maps at the desired retinal vascular layer (superficial, intermediate, or deep capillary plexus), the choriocapillaris, and the choroid.

A. Chang et al. (eds.), *Macular Surgery*, https://doi.org/10.1007/978-981-15-7644-7_4

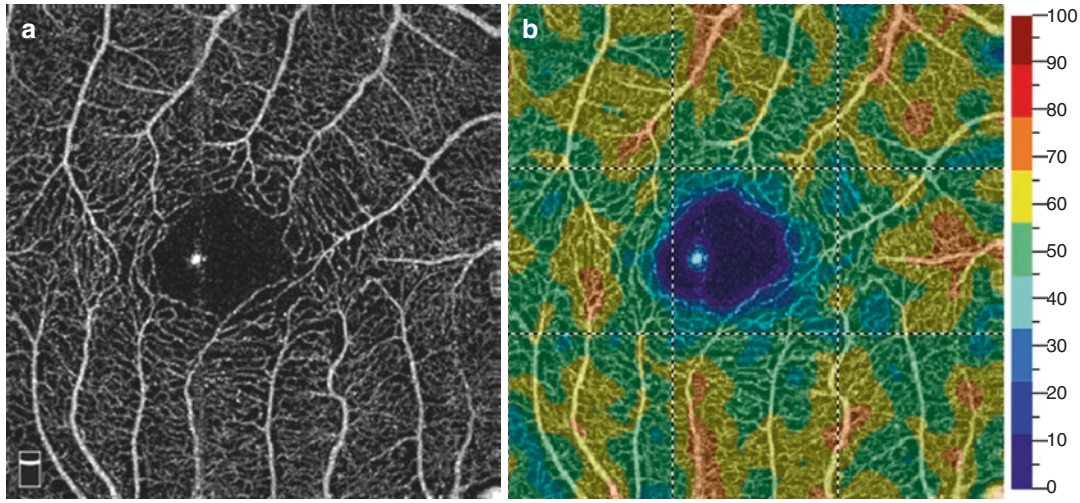

Fig. 4.1 OCTA of a normal eye. (**a**) 3 × 3 mm OCTA can. (**b**) Vessel density map of the same eye, showing the variations in vessel density, which are color-coded

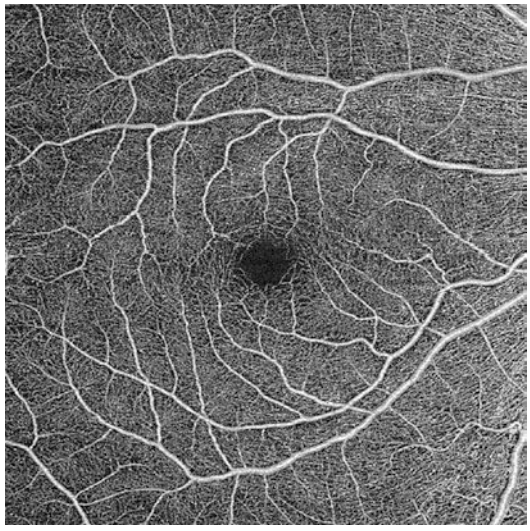

Fig. 4.2 6 × 6 mm OCTA scan of a normal eye

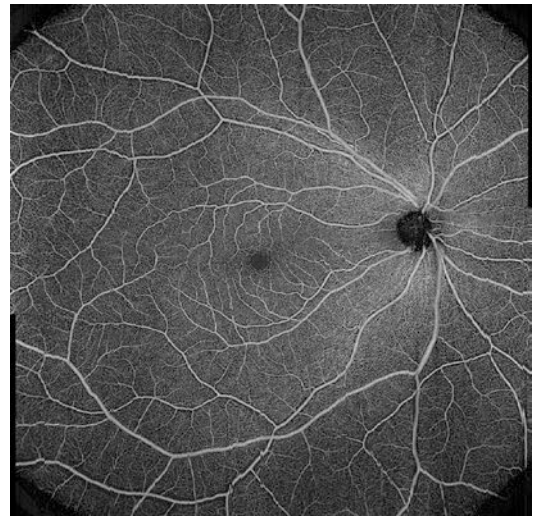

Fig. 4.3 15 × 15 mm OCTA scan of a normal eye, showing OCTA of the peripheral retina

These images can also be viewed cross-sectionally, allowing the reader to confirm the spatial location of any pathology which is seen on the en face images.

Various algorithms are used by different OCTA devices to calculate motion contrast. These algorithms detect motion perpendicular to the direction of the OCT beam using signal amplitude, signal phase, or both. Examples of algorithms include split spectrum amplitude decorrelation (SSADA), which uses OCT signal amplitude. SSADA was first demonstrated by Jia et al. [8] to improve image quality by reducing machine sensitivity to bulk eye motions as well as improving signal to noise ratio. SSADA generates a flow signal by measuring the speckle decorrelations between consecutive B-scans. The full OCT spectrum is split into multiple narrowband spectra, where decorrelation is calculated for each band before being averaged and combined to get the final flow signal. In this case, noise from bulk motion in the axial dimension is reduced without compromising flow signal from

the transverse dimension (retinal and choroidal flow). The downside of splitting the spectrum, however, is a reduction in axial resolution.

Other algorithms with clinical applications include speckle variance, phase variance, optical microangiography (OMAG), and correlation mapping [9, 10].

Speckle variance works to detect intensity (speckle) changes in OCT images [11–13]. Speckles are discrete areas of constructive interferences. When reflected off a moving object, the produced speckle will change more rapidly over time. Conversely, speckles reflected off stationary objects will not vary much with time. By measuring the amount of reflection at each voxel, the values of successive images measured at two different time points can be compared pixel by pixel. Large changes would typically correspond to the motion of erythrocytes in blood vessels [9, 14].

Another method for detecting motion contrast is to assess for phase variance or changes in the phase of the light waves. Moving erythrocytes will induce a variation in the phase of light reflected from one instant to the next, allowing for this to be measured. For moving erythrocytes, the variance will be much higher than in areas of no motion that show low variance from residual motion and Brownian movement.

OMAG uses both intensity and phase changes of the OCT signal to contrast blood for information [15]. OMAG improves differentiation between normal tissue and erythrocyte flow by modifying OCT hardware to introduce an externally imposed phase variation [9, 15, 16]. This helps counter the issue of bulk eye motion that phase-based detection was very sensitive to. OMAG has been implemented by the CIRRUS HD-OCT 5000 system with AngioPlex OCT angiography.

4.3 Advantages and Disadvantages of OCTA

Traditional methods of imaging vascular flow include dye-based angiography such as fluorescein angiography (FA) [17] and indocyanine green angiography (ICGA), [1–3] which require the injection of fluorescent dyes prior to imaging. FA and ICGA have been used in ophthalmology for decades and continue to play important roles in clinical practice. However, these imaging modalities have some limitations and disadvantages. Firstly, they are invasive and require intravenous access. They are contraindicated among patients with allergies to the dyes, and while these allergies are uncommon, the drugs may sometimes result in severe allergic reactions or even anaphylaxis. They are also time-consuming, requiring up to 45 minutes for the complete investigation, in order to visualize the different phases of the angiograms. FA and ICGA do not allow differentiation of vessels from different layers of the retina and choroid, respectively. Instead, the en face angiogram is a composite image of vessels from different vascular layers. This is especially evident in flash angiograms, where the choroid appears as a mass of overlapping vessels. While confocal scanning laser ophthalmoscopy, which is employed in devices such as the Heidelberg Spectralis, partially overcomes this by limiting light reflection from a specific tissue plane, it is still not possible to have depth resolution using these devices. Finally, the devices and/or drugs required for these investigations are not available in some centers or populations, thus limiting their applicability.

OCTA overcomes many of the limitations inherent in dye-based angiography. Firstly, OCTA is noninvasive, painless, and does not require contact with the patient. It does not require intravenous dye injection, hence eliminating the risk of allergic reactions. It is also much faster, taking a few minutes to perform, and hence more efficient in busy clinics. These advantages allow OCTA to be performed more frequently in patients, which makes it more suitable for close monitoring of patients. OCTA also provides depth resolution of the various vascular layers, which is unavailable with dye-based angiography. Moreover, it is possible to display both en face and cross-sectional images, allowing for flow within specific retinal and choroidal layers to be visualized and correlated with structural abnormalities. OCTA images are also not obscured by dye leakages seen in FA or ICGA and underlying diseased vessels can potentially be visualized.

However, OCTA does have several important limitations. OCTA is not able to demonstrate leakage from vessels. Unlike FA and ICGA, which demonstrate dynamic filling of the blood vessels, OCTA is a static image and the direction of blood flow cannot be determined using this modality alone. OCTA image data are dependent on the underlying OCTA instruments used. Algorithms may vary, and different machines have different protocols and processing methods, which may affect the appearance of the OCTA image. Hence, care is required when interpreting and comparing images from different machines. OCTA images can also be subject to different types of artifacts, leading to misinterpretation. These artifacts may be due to both technical and clinical factors and are discussed in detail in a subsequent section.

4.4 OCTA Vessel Density

OCTA en face images can be viewed qualitatively for the presence of abnormalities and can be further processed to produce quantitative, objective data on the vascular parameters. Objective metrics that have been described in reports include vessel density (Fig. 4.1b), vessel length density (skeletonized density), blood flow index, and fractal dimension.

Vessel density is defined as the percentage of the en face image that is occupied by retinal vessels [18]. Vessel density allows objective, quantitative measurements which facilitate comparison of OCTA scans and can potentially be used in further clinical trials.

Vessel density has been shown in several studies to vary with different physiological parameters. In a study by Wang et al. [19] that analyzed 105 normal patients, vessel density was shown to decrease with age. There were also gender differences, with the male sex correlating with higher densities of the superficial retinal plexus and the female sex correlating with higher densities of the deep retinal plexus. In another study by Mo et al. [20], macular, choriocapillaris, and radial peripapillary capillary densities (RPC) were measured and compared between groups of emmetropes, high myopes, and pathological myopes. Compared with the first two, pathological myopes had significantly decreased macular and RPC vessel densities. There was also a negative correlation seen between axial length and superficial, deep retinal, and RPC vessel densities.

Vessel density also has the potential for clinicians to differentiate between normal and pathological eyes. Superficial and deep retinal vessel densities have been shown to decrease in diabetic eyes even without retinopathy compared to healthy subjects [21]. In another study by Durbin et al. [22] comparing normal and diabetic subjects, vessel density measured in the superficial retinal layer had a high area under the receiver-operating characteristic curve; suggesting that it is an efficacious method for differentiating eyes with and without diabetic retinopathy. In this study, vessel density also correlated negatively with best-corrected visual acuity and severity of diabetic retinopathy.

Several studies have shown good reproducibility (inter and intraobserver) with the use of vessel density as a metric assuming the same machine, quantification algorithm, and angiocube size are used. In a study by Lei et al. [23], eyes from both healthy participants and patients with retinal diseases were examined with three different software versions of the same model of OCTA device (Cirrus HD-OCT model 5000; Carl Zeiss Meditec, Inc). Both vessel length density and perfusion density of the superficial retinal vasculature were shown to be obtained using high levels of repeatability and reproducibility. In this particular study, within each device (repeatability), the coefficient of variation (CV) ranged from 2.2 to 5.9% and 2.4 to 5.9% for vessel length density and perfusion density respectively, while the intraclass correlation coefficient (ICC) ranged from 0.82 to 0.98 and 0.83 to 0.95 for vessel length density and perfusion density, respectively. Among the three different software versions (reproducibility), the CV in all groups was less than 6%,

with the ICC ranging from 0.62 to 0.95. It is important to note, however, that vessel density measurements can vary significantly among various machines. Various OCTA devices use proprietary software with heterogeneous algorithms to binarize the OCTA images and calculate vessel density. Aside from using these machines to calculate vessel density, most studies export and post-process OCTA angiograms with different thresholding methods. This includes the use of the ImageJ algorithm and Otsu's algorithm [24–26].

4.5 Artifacts on OCTA

An important limitation of OCTA is the presence of artifacts. Artifacts may be a result of a multitude of factors, ranging from how the image data is being acquired, processed, and displayed, to the intrinsic properties of the eye being imaged. Artifacts are also common. In a study done by Falavarjani et al., at least one type of artifacts was seen in 89.4% of eyes imaged using OCTA [27]. These included banding, segmentation, and motion artifacts most commonly (89.4%, 61.4%, and 49.1%, respectively), as well as others such as unmasking, blink, vessel doubling, and out-of-window artifacts.

4.5.1 Low Signal Strength

Signal strength is influenced by the signal to noise ratio and are commonly influenced by pathologies as well as ocular factors. Low signals lead to difficulty in visualizing the smaller vessels of the eye that correspondingly produce smaller signals. Media opacities in the anterior segment, such as cataracts or corneal scars, may decrease the OCT signal. Other factors that decrease signal-to-noise ratio include dry eyes or incorrect position of the machine. In such situations, reimaging after lubrication or repositioning the patient may improve signal strength in some instances. Loss of signal strength may be global or focal. Global losses of signal strength include dense cataracts and vitreous hemorrhages. Focal losses of signal strength are due to focal opacities such as prominent vitreous floaters that obscure visualization of both the underlying retina and choroid or subretinal hemorrhage that obscures visualization of the underlying choroid.

While measures such as lubrication and repositioning may increase signal strength, approaches to reduce noise are often manufacturer specific.

4.5.2 Motion Artifacts

Eye movement during imaging is an important source of artifacts and can come from bulk eye movements, small saccades, or movement within the eye. For the latter, positional changes of the retina are often in the axial direction due to choroidal pulsation or intraocular pressure fluctuations.

Bulk eye movement often produces obvious shearing or gaps in en face images. In many machines, bulk eye movements are accounted for by active eye tracking. This works by measuring the position of the eye, with corrective measures taking place if the motion of the eye be greater than a selected threshold.

An approach to deal with artifacts from eye saccades and movement is a software-based approach developed by Kraus et al. [28]. This includes obtaining two OCT volumes from the same region—one in the horizontal and one in the vertical direction. These represent the same retinal structures but the effects of eye movements on these scans will be different and complementary.

Software-based methods work by estimating the amount of eye motion for each A-scan, translating the A-scan and then comparing the volumes. This software approach is intensive due to the number of A-scans needed. It should also be noted that while being able to correct movement artifacts, this software approach introduces artifacts on its own, such as loss of detail, vessel-doubling, image stretching, and quilting.

Other methods of account for eye movement would be to rescan portions affected by movement

with the rescanned image being stitched into the original image.

Software registration and correction complement active eye tracking and correct for some error that is not picked up by eye tracking. A study done by Camino et al. showed that a combination of eye tracking and software motion correction has been shown to reduce artifacts associated with software motion correction alone [29].

4.5.3 Projection Artifacts

During the imaging process, the OCT beam passes through overlying retinal structures to reach deeper layers. As it passes through the retina, the OCT beam may be reflected, absorbed, refracted, or scattered by these overlying structures leading to projection artifacts. For example, light may have varying fluctuations as it passes through flowing erythrocytes. These deeper structures may be illuminated by this fluctuating light even though these structures are stationary. Hence, a false impression of blood flow in these stationary structures may be given should they be deep to a blood vessel. The result of this would be the false detection of superficial vessels in the deeper layers of the retina. As such, it is no surprise that projection artifacts are seen in almost all images visualizing vessels at the level of the RPE. Several approaches to reduce projection artifacts have been investigated. One of the simplest would be to subtract the en face image of the superficial capillary plexus from the deeper layer.

4.5.4 Masking Defects

Masking defects arise from a process known as masking or thresholding. Masking describes the removal of OCTA data from structures with low signal or high amount of noise. This is important as areas with low signal can have the false appearance of flow due to random fluctuations of noise. However, this process of removing low signal results from the OCTA images makes it difficult to image flow deep in the choroid—an area of low signal especially if the RPE and choriocapillaris are intact. Hence, choroidal vessels underlying areas of intact RPE have little reflectivity and conversely, deep choroidal vessels can be visible in areas of RPE atrophy.

4.5.5 Segmentation Artifacts

In order to create en face images of the eye, different layers of the retina are selected, before summing up the vessel projected in these layers. Parameters such as reflectivity, texture, or continuity can be used to differentiate these layers, but are often less effective in pathological eyes that have distorted anatomy. Moreover, layer thickness varies from eye to eye and may be thinner, thicker, or even absent. In patients with pathological or high myopia, the presence of staphyloma may also lead to segmentation errors due to altered curvature. Incorrect segmentation can be identified and corrected by viewing the OCT B-scan images. However, this often is time-consuming and may be impractical to do for every imaged eye.

4.6 OCTA of the Normal Retinal Vasculature

Histological studies suggest three layers of capillary plexuses in the human retina—superficial vascular (SVP), intermediate capillary (ICP), and deep capillary plexuses (DCP) [30, 31]. While early OCTA studies describe only major vascular plexuses (superficial and deep vascular complexes), novel algorithms such as the 3-D projection artifact removal (PAR) may improve visualization of all the three capillary plexuses, in particular the ICP [32].

In a study done by Hirano et al. [33] eyes from 22 normal participants were examined using a full-spectrum, probabilistic OCTA, with and without 3-D PAR. In the study, en face

OCTA images of different vascular layers were described. Images of the SVP showed a centripetal branching pattern that terminated in a capillary ring around the foveal avascular zone. Comparing the ICP and DCP, DCP images reviewed vascular loops that were configured around a central point—much like a vortex. This central point is postulated by the authors to represent a vertical interconnecting vessel. This vortex-like configuration of vessels was not seen with the ICP.

4.7 OCTA of AMD

Optical coherence tomography angiography (OCTA) has become a useful tool in the management of age-related macular degeneration (AMD). The features detected on OCTA depend on the severity and spectrum of the disease. In addition to its roles in diagnosis and follow-up of nAMD, OCTA may also provide insights into the natural history and pathophysiology of the disease.

4.7.1 Non-Neovascular AMD

Non-neovascular or dry AMD is characterized by the presence of drusen which are yellow deposits located beneath the retinal pigment epithelium.

OCTA is useful in dry AMD to detect the presence of subclinical neovascularization in asymptomatic patients. This has been reported in up to 30% of patients with intermediate AMD [34]. These patients with subclinical CNV had an approximately 15 times greater risk of progressing to exudation compared to those without [35, 36].

The retinal pigment epithelium overlying the drusen may be highly reflective, which may cause projection artifacts from the overlying retinal vessels and giving the pseudo appearance of neovascularization [37]. As AMD progresses, OCTA shows measurable changes in signal void sizes in the choriocapillaris [37].

4.7.2 OCTA of the Choriocapillaris

OCTA is useful in imaging the choriocapillaris, where the dynamic nature of blood flow within the choriocapillaris allows detection of flow. By segmenting the RPE plus Bruch's membrane and projecting several micrometers below the RPE, a resultant en face OCTA image of the choriocapillaris is generated, which appears as a granular pattern of bright and dark areas [38–40]. Regions without flow signal (i.e., dark areas) are known as flow voids [37] and may represent either atrophic choriocapillaris vessels, vessels with a very slow flow rate that is slower than the device's sensitivity or may represent areas of shadowing arising from attenuation of OCT signal [41–43].

In healthy eyes, the number of flow voids increased with age and also with decreasing distance from the fovea [44–46]. Spaide described an increased number of choriocapillaris flow voids in normal eyes imaged with SD-OCTA with increasing age and a history of hypertension [45]. Utilizing SS-OCTA and a validated novel algorithm [47], Zheng et al. reported a positive correlation between decades of age and percentage of choriocapillaris flow deficits (FD%) which was consistent across the central and peripheral macula ($r > 0.50$ and $p < 0.001$ in all areas). The FD% increase was found to be the greatest in the central 1-mm circular area centered on the macula and smallest in the 2.5-mm rim in the peripheral retina [46].

Among eyes with geographic atrophy, flow voids were significantly increased compared with age-matched controls [48]. Additionally, Rinella et al. reported that the number of flow voids in the periphery of the atrophic regions (within 2° of GA) was found to be significantly greater compared to areas away (outside 2° of GA) [48]. Flow voids were also reported to be significantly increased in eyes with choroidal neovascularization (CNV) compared to age-similar normal controls. (20.56 ± 4.95, 95% CI: 17.64–23.49 vs. 10.95 ± 2.08, 95% CI: 9.73–12.18, respectively; $P = 0.0001$) which also correlated positively with CNV lesion area ($r = 0.84$; 95% CI: 0.49–0.96; $P = 0.001$) [42].

4.7.3 Exudative AMD

For many decades, the diagnosis and classification of exudative AMD have been made using fluorescein angiography (FA). However, FA is associated with some disadvantages, such as its invasive nature and the potential for allergic reactions caused by fluorescein dye. OCTA overcomes these limitations. It has been reported to be able to show between 75 and 90% of the flow patterns as seen on FA [49, 50].

4.7.3.1 Type 1 CNV

OCTA has been reported to detect between 67 and 100% of type 1 choroidal neovascularizations [50–52]. There is better visualization of the vascular structures in Type 1 CNV on OCTA compared to FA because there is less masking from the overlying retina pigment epithelium and the absence of obscuration from dye leakage [53].

On cross-sectional OCTA, intrinsic flow is seen within the pigment epithelial detachment in the sub-RPE space. On the corresponding en face OCTA, CNV lesions can be visualized as a well-defined network or tangle of vessels lying between the RPE and the Bruch's membrane [54]. Trunk vessels may be present. The choriocapillaris in the region beneath and around the CNV may show some signs of loss. Chronic CNV lesions may also exhibit a network of tiny capillaries around the CNV border with a lack of mature dilated feeder vessels [55].

4.7.3.2 Type 2 CNV

On cross-sectional OCTA, an active type 2 CNV lesion is seen as subretinal hyperreflective material above the RPE with intrinsic flow signals (Fig. 4.4). Hyperflow patterns detected (often described as glomerulus or medusa shaped) are associated with a thicker main vessel branch connected to the deeper choroid. In some cases, this high flow signal may cause a projection artifact onto the deeper choriocapillaris layer. A dark halo may be seen around the lesion and this was postulated to correspond to masking from surrounding blood, exudation, or subretinal fibrosis [56, 57].

On the corresponding en face scans, type 2 CNV is seen as a network of vessels in the normally avascular outer retina [58] These vascular networks often have a lacy pattern with uniform intensity but variable caliber. The CNV lesions detected on OCTA correlate closely with the area of leakage on FFA and are generally more distinct compared to ICGA [59]. Similar to type 1 CNV, the choriocapillaris surrounding the CNV may show some signs of loss and trunk vessels may be present.

An added benefit of OCTA is the identification of both the superficial subretinal type 2 component and the deeper sub-RPE type 1 component by varying the depth of segmentation.

4.7.3.3 Type 3 CNV

Cross-sectional OCTA of type 3 CNV showed two patterns of flow: [60].

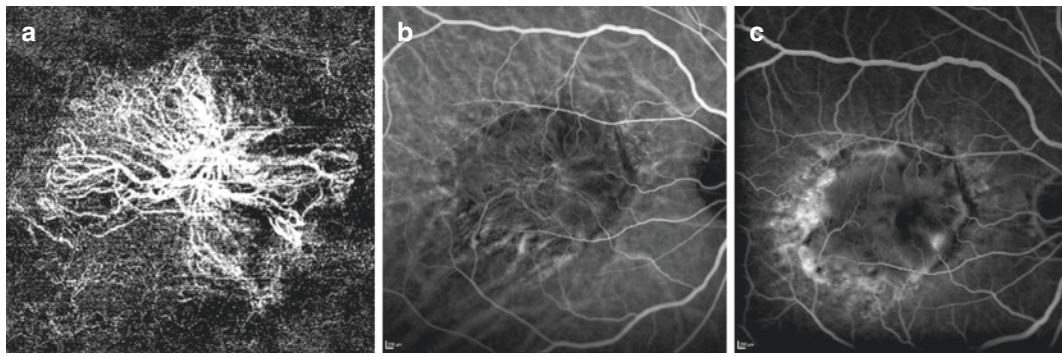

Fig. 4.4 Neovascular age-related macular degeneration. (**a**) OCTA demonstrating the CNV lesion. (**b**) Indocyanine green angiogram at 3 min, showing the CNV vessels. The overlying retinal vessels as well as the large choroidal vessels are visible. (**c**) Fluorescein angiogram showing occult leakage

1. Discrete intraretinal flow signal or
2. Linear flow signal extending from the intraretinal areas through to the RPE band

The en face OCTA shows a discrete bright tuft of microvessels with high flow extending from the middle retinal layers or deep capillary plexuses into the deep retina and, occasionally, past the RPE [60]. As the type 3 CNV develops over time, these vessels anastomose with the deep retinal capillary plexuses and extend into the outer retina and eventually into the sub-RPE space [60]

4.7.4 Sensitivity and Specificity

Compared with FA, OCTA has a sensitivity of 50–100% and a specificity of 79–91% [51, 61, 62]. In some studies where when structural OCT was used together with OCTA data, the sensitivity increased to 87% [61].

4.7.5 Use of OCTA in Management of AMD

4.7.5.1 Active or Inactive MNV

Since OCTA may detect incidental findings of neovascularization in patients who are asymptomatic and appear clinically to have non-neovascular AMD, it is imperative to determine if treatment is indicated. There are some reports on characteristics of the CNV lesion on OCTA, as well as correlating with structural OCT, which can help clinicians determine the activity levels of such lesions and the need for treatment. Examples of such features include:

Active CNV:

1. Presence of fine vessels at the edge of the neovascularization.
2. Peri-lesional dark halo.
3. Extensive vascularity.
4. Appearance of anastomoses and loops,
5. Well-defined shape (lacy wheel or sea-fan shaped) [63].

Inactive CNV:

1. Large vessels which have the appearance of a "dead tree" [63].
2. Paucity of fine branching vessels [63].
3. Absence of anastomoses, loops, and peripheral arcades.
4. Paucivascular fibrotic scar.

4.7.5.2 Monitoring of Treatment Efficacy

OCTA provides both quantitative and qualitative evaluation of MNV and hence is an useful and powerful tool for monitoring and follow-up of MNV.

Following treatment with anti-VEGF agents, neovascularization has been shown to decrease in size as well as density due to the loss of finer vessels along the border and within the CNV [64, 65]. This regression is maximal around 1–2 weeks following treatment [64].

Chronic CNV lesions may show little anatomical response to anti-VEGF and the lesion area and vessel density may remain unchanged. These may eventually develop a pruned tree appearance, which is an indicator of inactivity [54].

4.7.6 Limitations and Pitfalls in Diagnosing MNV on OCTA

Projection artifacts from the superficial retinal vasculature can give the erroneous appearance of neovascularization in a normal eye [66]. Other retinal elevations such as drusen, serous, and drusenoid pigment epithelial detachments as well as scars can also affect the segmentation of retinal layers and give the false appearance of neovascularization.

In patients with macular atrophy and loss of the choriocapillaris, the larger choroidal vessels may appear within the choriocapillaris slab. These may appear similar to neovascularization.

This illustrates that it is important to assess the OCT B-scan to correlate the presence of flow with the appearance of the en face image. It is also useful to perform careful mapping of the vessels as well as confirming the location of these

vessels beneath the Bruch's membrane. This will help to differentiate the normal vessels from neovascularization.

4.8 OCTA of Polypoidal Choroidal Vasculopathy (PCV)

Polypoidal choroidal vasculopathy (PCV) is characterized by the presence of polypoidal lesions together with a branching vascular network (BVN) that supplies these lesions. This condition occurs more commonly among some populations, such as Asians [67, 68]. Currently, ICGA is the gold standard for diagnosing PCV [1, 3, 69, 70], although color fundus photography, multicolor imaging, and FA [6, 7] can identify features which are suggestive of PCV. OCTA provides a complementary diagnostic tool to ICGA in diagnosing PCV with the sensitivity of OCTA in detecting PCV ranging from 39.5 to 43.9% and the specificity varying from 79.1 to 87.1% [68, 71].

4.8.1 Polypoidal Lesions

The polypoidal lesions exhibit variability in their flow characteristics and structure, with some appearing as hyperflow round structures (Fig. 4.5) with a hypointense halo and up to 75% appearing as hypoflow round structures. Hyperflow lesions tended to be less pulsatile and to have a thicker subfoveal choroid. The round structures were

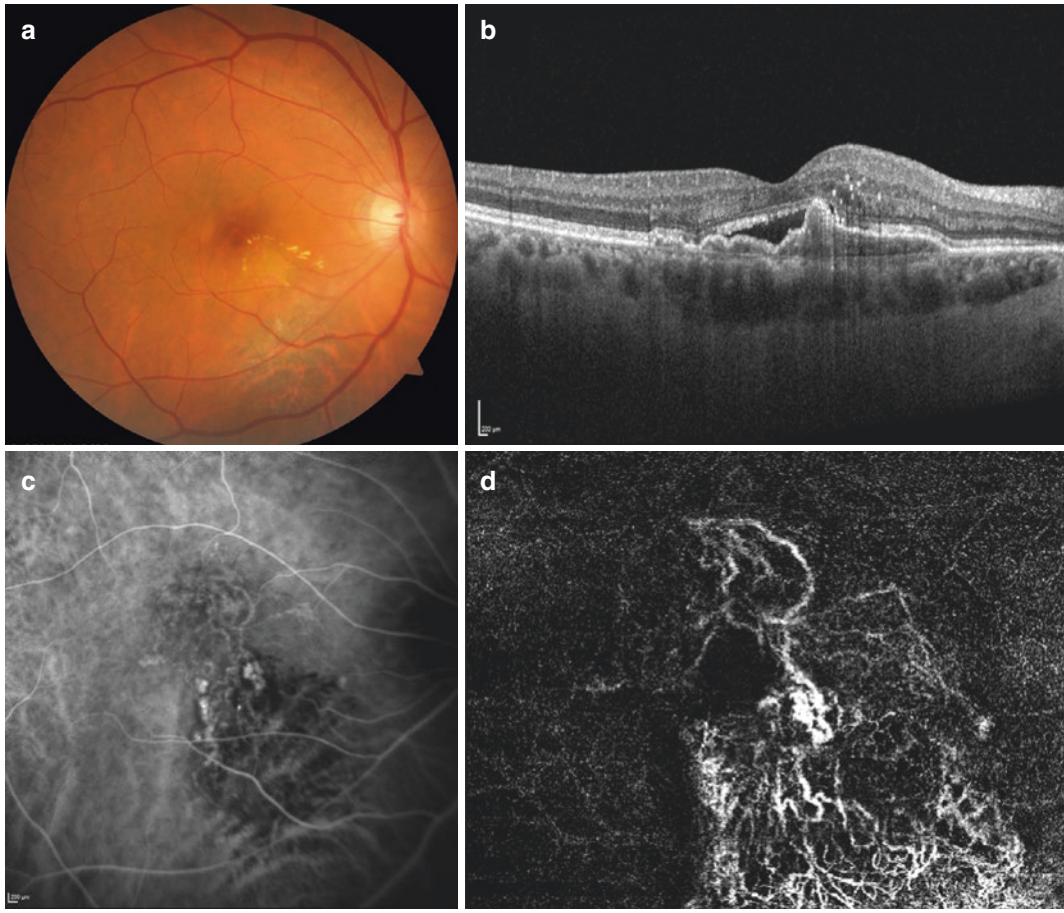

Fig. 4.5 Polypoidal choroidal vasculopathy (PCV). (**a**) Color fundus photograph, showing mottling and thinning of the retina inferiorly. (**b**) OCT B-scan showing elevation of the retinal pigment epithelium, corresponding to the polypoidal lesion. Subretinal fluid is observed. (**c**) Indocyanine green angiogram showing polypoidal lesions and the associated branching vascular network. (**d**) OCTA illustrating the polypoidal lesion and branching vascular network

typically situated at the termini of the vascular network. These polypoidal structures were mainly above the Bruch's membrane within the dome of the RPE detachment, with the choroidal stalks extending deeper in the choroid layer.

However, OCTA is only able to detect 17–85% of polyps compared to ICGA. It is believed that the absence of lesions on OCTA may be related to slow or turbulent flow within the polypoidal lesions.

In contrast to the BVN, the rate of polyp progression was highly variable ranging from 17 to 85% [72–75].

4.8.2 Branching Vascular Membranes (BVNs)

The BVN is detected using OCTA in between 77.8 and 100% of eyes with PCV. It is visualized as a hyperflow lesion, located between the RPE and Bruch's membrane [73, 76]. This vascular net was variable in size but correlated closely with the location and shape seen on the ICGA. Often, en face OCTA of the BVN showed networks of vessels in much more detail than ICGA.

In one study, 70.9% of the PCV cases (22/31) had clear or obvious BVNs and that this feature was the most sensitive to make an accurate diagnosis (sensitivity 97.5%). The sensitivity increased from 69.5 to 90% after OCTA [77].

Following treatment with anti-VEGF and PDT, reduction in flow within the PCV complexes in most eyes is expected. However, despite significant improvement in exudation, the vascular network may remain unchanged. Early recurrence of PCV may be detected on OCTA via changes in the appearance of the vascular network as well as the presence of persistent flow signals within the vascular network.

4.9 OCTA of Retinal Vascular Diseases

4.9.1 Diabetic Retinopathy

The prevalence of diabetes mellitus is increasing in many parts of the world and, with it, the frequency of ocular complications such as diabetic retinopathy and diabetic macular edema. Previously, FA was required to assess the presence and extent of retinal non-perfusion and to neovascularization at the disc and elsewhere. Due to the requirement for venous access and the use of intravenous dye injections, this investigation could not be performed frequently. In contrast, the convenience of OCTA allows more frequent reviews of eyes with diabetic eye disease and also provides new insights due to the ability to segment different vascular plexuses in the retina.

OCTA is able to detect microaneurysms [78–81], which is the hallmark of diabetic retinopathy. Unlike FA, where microaneurysms typically appear as round dots, OCTA can differentiate various shapes in microaneurysms, including solid round lesions, round lesions with dark centers, or fusiform lesions [81]. It is important, however, to note that there is incomplete agreement between FA and OCTA in terms of the number and locations of microaneurysms. Studies have reported that a greater number of microaneurysms are detected using FA compared to OCTA and it has been suggested that the histology of microaneurysms could potentially result in turbulent or slower blood flow, the velocity of which is below the slowest detectable flow using current OCTA devices [79, 80]. Parravano et al. reported varying detection rates of microaneurysms on OCTA depending on their internal reflectivity on spectral-domain OCT. They found that microaneurysms with hyporeflectivity on OCT had a lower detection rate on OCTA, compared to those with moderate or hyperreflectivity [82].

Retinal neovascularization at the optic disc or elsewhere can be detected using OCTA [79, 80, 83]. By setting the segmentation of the OCTA slab above the internal limiting membrane, blood flow through these new vessels can be detected. OCTA is advantageous in that it is not affected by leakage, unlike FA where leakage from the neovascularization can obscure image details in later phases of the angiogram.

Another feature in eyes with diabetic retinopathy which can be detected using OCTA are looping vessels with increased caliber adjacent to areas of impaired capillary perfusion [78, 81]. In

some cases, these are consistent with clinically defined intraretinal microvascular abnormalities, which is a feature of more advanced diabetic retinopathy [81]. Other features, such as dilated capillary segments [78] and clustered or tortuous capillaries [78], also illustrate the underlying features associated with retinal vascular diseases.

Since diabetes mellitus affects the microvasculature in the eye, it is not surprising that eyes with diabetic retinopathy will manifest with areas of retinal non-perfusion and capillary dropout (Fig. 4.6). These can be identified using both FA and OCTA, however, OCTA has the additional advantage of being able to resolve different vascular plexuses in the retina, thus illustrating the areas of non-perfusion in the superficial, intermediate, and deep capillary plexuses [78–81, 83, 84]. Studies have reported that the area of retinal non-perfusion differs between the superficial and deep retinal plexuses [80, 85, 86]. The area of retinal non-perfusion increases with the severity of diabetic retinopathy [84, 87]. Besides the reduction in blood flow in the retinal circulation, studies have also reported regionals of flow impairment in the choriocapillaris among patients with non-proliferative and proliferative diabetic retinopathy [78].

Changes occur at the foveal avascular zone (FAZ) in diabetics, with both more irregularity of the FAZ and enlargement of this region. OCTA of normal eyes demonstrates a range of FAZ sizes and circularity (the extent to which the FAZ resembles a perfect circle) [88]. Using OCTA, increasing irregularity of the FAZ has been identified in eyes of diabetics, with gaps and interruptions of the capillary networks [85, 89, 90]. The size of the FAZ is larger among eyes with diabetic retinopathy compared to those without [83, 86, 91, 92]. This difference appears to be more pronounced in the deep capillary plexus [89, 90].

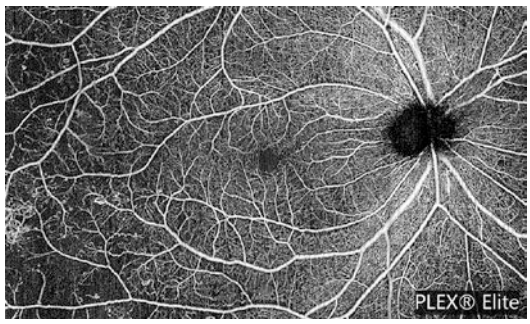

Fig. 4.6 Diabetic retinopathy. OCTA of the superficial retinal plexus, showing capillary dropout which is more severe in the temporal periphery

Retinal vessel density is a measure of the amount of flow within a region of an OCTA scan. Studies comparing eyes of diabetics with normal controls have reported that eyes of diabetics have reduced vessel densities compared to normal controls [21, 79, 86, 87]. This reduction is evident even among eyes of diabetics with no clinical features of diabetic retinopathy and becomes more severe as the severity of diabetic retinopathy worsens [87]. The reduction in vessel density with diabetic retinopathy is observed in both the superficial and deep capillary plexuses [21, 83, 86, 87]. Local reductions in vascular density of the deep capillary plexus have been shown to correlate with regions of disorganization of the retinal inner layers (DRIL), which are demonstrated on OCT B-scans [37, 93].

Changes in vessel density may serve as useful biomarkers for early detection of diabetic retinopathy and to indicate the potential for progression. Studies have reported significant correlations between systolic blood pressure and ocular perfusion pressure and the vessel density in the deep retinal plexus in patients with non-proliferative diabetic retinopathy [21].

An important consideration when using OCTA to assess for features of diabetic retinopathy is that the disease can occur throughout the retina and may not be localized in a specific region. Hence, the field of view of the OCTA scan is an important consideration. Investigators have reported that a wider field of view on the OCTA was useful for detecting the full extent of vascular changes as well as capillary non-perfusion [83]. This is especially important when considering that studies of ultra-widefield FA in patients with retinal vascular diseases have identified significant regions of retinal non-perfusion in the peripheral retina [4, 5].

4.9.2 Diabetic Macular Edema

Although the features of diabetic macular edema (DME) are seen on structural OCT, studies have described some findings on OCTA associated with this condition. Microaneurysms are associated with DME and occur with higher density in the deep capillary plexus compared to the superficial capillary plexus (1.71/mm^2 vs. 0.17/mm^2, $P < 0.001$) [94].

OCTA scans also show dark regions devoid of flow signal which correspond to the presence of intraretinal cysts [37, 81, 85, 95]. These are usually oval or oblong in shape, with smooth borders and do not follow the distribution of the surrounding capillaries [95]. It is believed that these may result from spaces with low perfusion, blockage of signal from the vessels caused by the presence of intraretinal fluid or due to displacement of the retinal vessels caused by the edema [95].

Intraretinal cysts and fluid may also manifest with extravascular signals, which are seen on en face OCTA images. "Suspended scattering particles in motion (SSPiM)" is a relatively novel imaging feature of retinal vascular diseases, including DME, which are detected on OCTA [96]. SSPiM represents an extravascular OCTA signal which is related to varying degrees of hyperreflective material seen on structural OCT. It is believed that these are due to Brownian motion of particles within the intraretinal fluid, which appears as flow on OCTA B-scans [96].

Eyes with both diabetic retinopathy and DME have been reported to have significantly lower vascular flow density in the deep capillary plexus compared to eyes with diabetic retinopathy but no DME (13.23% vs. 20.75%, $p < 0.001$) [97]. In contrast, there was no statistically significant difference in vascular flow density in the superficial layer. Following treatment with anti-VEGF agents, patients with poor treatment response showed lower vessel density, more microaneurysms, and a larger FAZ in the deep capillary plexus compared to those who responded favorably [97].

4.9.3 Retinal Vein Occlusion

Among patients with retinal vein occlusion, OCTA is useful in detecting the extent of vascular non-perfusion, which occurs in both the superficial and deep capillary plexuses (Fig. 4.7) [98, 99]. Similar to diabetic retinopathy, the FAZ may be enlarged in both the superficial and deep vascular plexuses [99].

OCTA also detects evidence of capillary changes [98, 100], such as dilation, pruning,

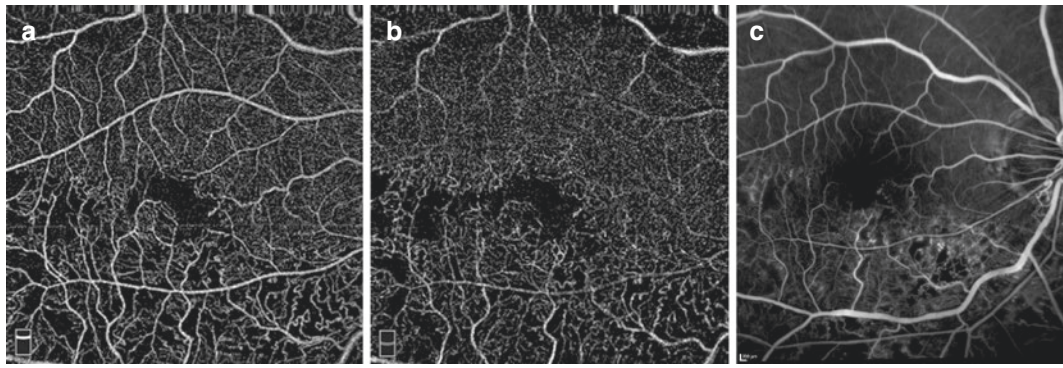

Fig. 4.7 Branch retinal vein occlusion. (**a**) OCTA of the superficial retinal plexus, showing capillary dropout inferiorly. The foveal avascular zone outline is irregular. (**b**) OCTA of the deep retinal plexus, showing the capillary dropout affecting the inferior retina. (**c**) Fluorescein angiogram, illustrating the capillary dropout in the retina. The FAZ is less well demarcated compared to the OCTA

telangiectasia, and vascular dilation, as well as the presence of shunt vessels [98] and retinal neovascularization [100]. Among patients with retinal vein occlusion, cystoid spaces occur more commonly in the deep compared to the superficial retinal plexus [101].

Paracentral acute middle maculopathy (PAMM) refers to band-like hyper-reflective lesions which are mostly confined to the inner nuclear layer visualized on SD-OCT. [102] Initially described by Sarraf et al. as a variant of acute macular neuroretinopathy [102], it is now understood to be a clinical finding associated with ischemia or infarction of the deep vascular complex (intermediate and deep retinal capillary plexus) [103]. PAMM has been reported to be associated with a large spectrum of retinal vascular disorders and systemic conditions [103–107]. Bakhoum et al. described a distinct progression of PAMM pattern progression on SD-OCT, pointing toward an ischemic cascade occurring in the parafoveal region in eyes with retinal vascular occlusion. The authors found that the ischemia occurred in the parafoveal macula, initially developing at the venular pole of the deep capillary plexus (manifesting as perivenular fern-like PAMM in the INL), which progresses laterally through the INL (manifesting as globular PAMM in the INL), and then anteriorly into the inner retina at the level of the superficial capillary plexus (SCP), with worsening visual acuity in each stage [108]. This anterior progression of ischemia implies a serial organization of the retinal capillary plexuses [109].

Unlike fluorescein angiography, OCTA's ability to produce detailed, high-resolution images of the retinal vasculature segmented by layer [37] has allowed for the correlation of PAMM with attenuation and pruning of the DCP visualized on the OCTA in multiple studies [67, 103, 104, 106, 110, 111]. While no study has reproduced Bakhoum et al.'s findings of a distinct PAMM ischemic cascade on OCTA, a recent study by Maltsev et al. described a tendency for resolved PAMM lesions, defined as INL thinning with OPL elevation, to localize paravascularly in majority of BRVO and CRVO patients [112].

4.9.4 Retinal Artery Occlusion

In patients with retinal artery occlusion, OCTA is useful in detecting the presence of macular ischemia and vascular flow changes, which may occur in both the superficial and deep capillary plexuses. These typically correspond to regions of delayed perfusion seen on FA [113]. In some eyes, perfusion of the deep capillary plexus may be maintained in areas of persistent ischemia in the superficial plexus [113]. In addition, there may be attenuation of the radial peripapillary capillaries, which correspond to thinning of the retinal nerve fiber layer [113].

4.10 OCTA in Inflammatory Conditions and Inherited Retinal Dystrophies

OCTA has been shown to be useful for evaluating the choroidal and retinal blood flow among patients with inherited retinal dystrophies and inflammation, including Stargardt disease, retinitis pigmentosa, Best vitelliform macular dystrophy, and choroideremia [114]. Areas of hypoperfusion and vascular insufficiency are well demonstrated in these conditions.

In addition, OCTA can detect neovascularization occurring in diseases of the retina and choroid, including inherited retinal dystrophies and inflammatory conditions [115–118]. The CNV lesions more clearly seen on OCTA compared to other imaging modalities such as FA [114]. In a study of ten eyes with multifocal choroiditis, OCTA identified all CNV lesions [115]. Active CNV lesions were found to have well-circumscribed margins, interlacing shapes, and a surrounding dark ring. In contrast, inactive CN lesions had poorly circumscribed margins, tangled shapes, and a "dead tree" appearance, with the surrounding dark ring appearing less frequently [115].

In patients with Stargardt disease, decreased vessel densities in the superficial and deep retinal plexuses, and the choriocapillaris, have

been demonstrated using OCTA. In addition, the superficial FAZ was found to be larger than normal controls [114, 119]. In a study of consecutive patients with Stargardt disease, quantitative parameters such as vessel density, vessel tortuosity, vessel dispersion, and vessel rarefaction were significantly worse than normal controls [120]. A study comparing OCTA of patients with Stargardt disease and AMD found greater areas of rarefaction of the choriocapillaris flow signal in Stargardt disease compared to AMD [121].

Different patterns of choroidal hypoperfusion were reported on OCTA among patients with white dot syndromes [122]. For patients with presumed ocular histoplasmosis syndrome and multiple evanescent white dot syndrome, choroidal hypoperfusion correlated well with clinical pathology. In contrast, regions of choroidal hypoperfusion were more widespread in both acute posterior multifocal placoid pigment epitheliopathy (APMPPE) and birdshot chorioretinopathy. One study reported that the resolution of choroidal hypoperfusion in APMPPE preceded the resolution of photoreceptor abnormality and visual recovery [123]. This suggests that the pathophysiology of APMPPE likely involves a primary hypoperfusion of the inner choroid with resultant RPE and photoreceptor abnormality and vision loss [123].

In Best vitelliform macular dystrophy, OCTA was shown to be superior to FA in detecting CNV because of masking of the CNV on FA by the vitelliform material [124]. In addition, the majority of patients had abnormal FAZ in the superficial and deep FAZ with patchy loss of vascularity in both retinal plexuses [124].

4.11 Conclusion

OCTA has changed the practice of ophthalmology, especially in the diagnosis, monitoring, and management of retinal diseases. Its noninvasive nature, rapid scanning time, and ability to segment different vascular layers have proved invaluable to understanding the pathophysiology of retinal diseases. It is important, however, to understand the current limitations and pitfalls of this modality.

Acknowledgments *Financial disclosures*: Colin S. Tan—Research Support from National Medical Research Council Transition Award (NMRC/TA/0039/2015) and NMRC Centre Grant (CG) Programme (CGAug16M012). Conference support from Bayer and Novartis.

SriniVas R. Sadda—Consultant for Allergan, Genentech, Roche, Novartis, Iconic, Thrombogenics, Centervue, Heidelberg, Optos and Carl Zeiss Meditec. Research Support from Allergan, Genentech, Optos, and Carl Zeiss Meditec.

References

1. Tan CS, Ngo WK, Chen JP, et al. EVEREST study report 2: imaging and grading protocol, and baseline characteristics of a randomised controlled trial of polypoidal choroidal vasculopathy. Br J Ophthalmol. 2015;99:624–8.
2. Tan CS, Ngo WK, Lim LW, et al. EVEREST study report 3: diagnostic challenges of polypoidal choroidal vasculopathy. Lessons learnt from screening failures in the EVEREST study. Graefes Arch Clin Exp Ophthalmol. 2016;254:1923–30.
3. Tan CS, Ngo WK, Lim LW, Lim TH. A novel classification of the vascular patterns of polypoidal choroidal vasculopathy and its relation to clinical outcomes. Br J Ophthalmol. 2014;98:1528–33.
4. Singer M, Tan CS, Bell D, Sadda SR. Area of peripheral retinal nonperfusion and treatment response in branch and central retinal vein occlusion. Retina. 2014;34:1736–42.
5. Tan CS, Chew MC, van Hemert J, et al. Measuring the precise area of peripheral retinal non-perfusion using ultra-widefield imaging and its correlation with the ischaemic index. Br J Ophthalmol. 2016;100:235–9.
6. Tan CS, Ting DS, Lim LW. Multicolor fundus imaging of polypoidal choroidal vasculopathy. Ophthalmol Retin. 2019;3(5):400–9. https://doi.org/10.1016/j.oret.2019.01.009.
7. Tan CS, Ting DS, Lim LW. Multicolour imaging for the detection of polypoidal choroidal vasculopathy and age-related macular degeneration. Clin Exp Ophthalmol. 2019;47:621–30.
8. Jia Y, Tan O, Tokayer J, et al. Split-spectrum amplitude-decorrelation angiography with optical coherence tomography. Opt Express. 2012;20:4710.
9. Chen C-L, Wang RK. Optical coherence tomography based angiography [Invited]. Biomed Opt Express. 2017;8:1056.

10. McNamara PM, Subhash HM, Leahy MJ. In vivo full-field en face correlation mapping optical coherence tomography. J Biomed Opt. 2013;18:126008.
11. Conroy L, DaCosta RS, Vitkin IA. Quantifying tissue microvasculature with speckle variance optical coherence tomography. Opt Lett. 2012;37:3180.
12. Mahmud MS, Cadotte DW, Vuong B, et al. Review of speckle and phase variance optical coherence tomography to visualize microvascular networks. J Biomed Opt. 2013;18:50901.
13. Mariampillai A, Leung MKK, Jarvi M, et al. Optimized speckle variance OCT imaging of microvasculature. Opt Lett. 2010;35:1257.
14. Spaide RF, Fujimoto JG, Waheed NK, et al. Optical coherence tomography angiography. Prog Retin Eye Res. 2018;64:1–55.
15. Wang RK, Jacques SL, Ma Z, et al. Three dimensional optical angiography. Opt Express. 2007;15:4083.
16. Huang Y, Zhang Q, Thorell MR, et al. Swept-source OCT angiography of the retinal vasculature using intensity differentiation-based optical microangiography algorithms. Ophthalmic Surg Lasers Imaging Retin. 2014;45:382–9.
17. Tan CS, Ngo WK, Lim LW, et al. EVEREST study report 4: Fluorescein angiography features predictive of polypoidal choroidal vasculopathy. Clin Exp Ophthalmol. 2019;47:614–20.
18. Rabiolo A, Gelormini F, Sacconi R, et al. Comparison of methods to quantify macular and peripapillary vessel density in optical coherence tomography angiography. PLoS One. 2018;13:e0205773.
19. Wang Q, Chan S, Yang JY, et al. Vascular density in retina and choriocapillaris as measured by optical coherence tomography angiography. Am J Ophthalmol. 2016;168:95–109.
20. Mo J, Duan A, Chan S, et al. Vascular flow density in pathological myopia: an optical coherence tomography angiography study. BMJ Open. 2017;7:e013571.
21. Dimitrova G, Chihara E, Takahashi H, et al. Quantitative retinal optical coherence tomography angiography in patients with diabetes without diabetic retinopathy. Invest Opthalmology Vis Sci. 2017;58:190.
22. Durbin MK, An L, Shemonski ND, et al. Quantification of retinal microvascular density in optical coherence tomographic angiography images in diabetic retinopathy. JAMA Ophthalmol. 2017;135:370–6.
23. Lei J, Durbin MK, Shi Y, et al. Repeatability and reproducibility of superficial macular retinal vessel density measurements using optical coherence tomography angiography en face images. JAMA Ophthalmol. 2017;135:1092.
24. Devarajan K, Di Lee W, Ong HS, et al. Vessel density and En-face segmentation of optical coherence tomography angiography to analyse corneal vascularisation in an animal model. Eye Vis. 2019;6:2.
25. Lauermann JL, Eter N, Alten F. Optical coherence tomography angiography offers new insights into choriocapillaris perfusion. Ophthalmologica. 2018;239:74–84.
26. Nicolò M, Rosa R, Musetti D, et al. Choroidal vascular flow area in central serous chorioretinopathy using swept-source optical coherence tomography angiography. Investig Ophthalmol Vis Sci. 2017;58:2002–10.
27. Ghasemi Falavarjani K, Al-Sheikh M, Akil H, Sadda SR. Image artefacts in swept-source optical coherence tomography angiography. Br J Ophthalmol. 2017;101:564–8.
28. Kraus MF, Potsaid B, Mayer MA, et al. Motion correction in optical coherence tomography volumes on a per A-scan basis using orthogonal scan patterns. Biomed Opt Express. 2012;3:1182.
29. Camino A, Zhang M, Gao SS, et al. Evaluation of artifact reduction in optical coherence tomography angiography with real-time tracking and motion correction technology. Biomed Opt Express. 2016;7:3905–15.
30. Henkind P. Radial peripapillary capillaries of the retina. I. Anatomy: human and comparative. Br J Ophthalmol. 1967;51:115–23.
31. Tan CSH, Cheong KX. Macular choroidal thicknesses in healthy adults—relationship with ocular and demographic factors. Investig Opthalmol Vis Sci. 2014;55:6452.
32. Garrity ST, Iafe NA, Phasukkijwatana N, et al. Quantitative analysis of three distinct retinal capillary plexuses in healthy eyes using optical coherence tomography angiography. Investig Ophthalmol Vis Sci. 2017;58:5548–55.
33. Hirano T, Chanwimol K, Weichsel J, et al. Distinct retinal capillary plexuses in normal eyes as observed in optical coherence tomography angiography axial profile analysis. Sci Rep. 2018;8:1–7.
34. Carnevali A, Cicinelli MV, Capuano V, et al. Optical coherence tomography angiography: a useful tool for diagnosis of treatment-naïve quiescent choroidal neovascularization. Am J Ophthalmol. 2016;169:189–98.
35. de Oliveira Dias JR, Zhang Q, Garcia JMB, et al. Natural history of subclinical neovascularization in nonexudative age-related macular degeneration using swept-source OCT Angiography. Ophthalmology. 2018;125(2) Elsevier Inc.:255–66.
36. Hanutsaha P, Guyer DR, Yannuzzi LA, et al. Indocyanine-green videoangiography of drusen as a possible predictive indicator of exudative maculopathy. Ophthalmology. 1998;105:1632–6.
37. Spaide RF. Volume-rendered optical coherence tomography of diabetic retinopathy pilot study. Am J Ophthalmol. 2015;160:1200–10.
38. Braaf B, Vermeer KA, Vienola KV, de Boer JF. Angiography of the retina and the choroid with phase-resolved OCT using interval-optimized backstitched B-scans. Opt Express. 2012;20:20516.
39. Choi WJ, Mohler KJ, Potsaid B, et al. Choriocapillaris and choroidal microvasculature

imaging with ultrahigh speed OCT angiography. PLoS One. 2013;8(12):e81499.
40. Sohrab M, Wu K, Fawzi AA. A Pilot study of morphometric analysis of choroidal vasculature in vivo, using en face optical coherence tomography. PLoS One. 2012;7:e48631.
41. Cole ED, Novais EA, Louzada RN, et al. Visualization of changes in the choriocapillaris, choroidal vessels, and retinal morphology after focal laser photocoagulation using OCT angiography. Investig Ophthalmol Vis Sci. 2016;57:OCT356–61.
42. Keiner CM, Zhou H, Zhang Q, et al. Quantifying choriocapillaris hypoperfusion in patients with choroidal neovascularization using swept-source OCT angiography. Clin Ophthalmol. 2019;13:1613–20.
43. Mullins RF, Johnson MN, Faidley EA, et al. Choriocapillaris vascular dropout related to density of drusen in human eyes with early age-related macular degeneration. Investig Ophthalmol Vis Sci. 2011;52:1606–12.
44. Nassisi M, Baghdasaryan E, Tepelus T, et al. Topographic distribution of choriocapillaris flow deficits in healthy eyes. PLoS One. 2018;13(11):e0207638.
45. Spaide RF. Choriocapillaris flow features follow a power law distribution: implications for characterization and mechanisms of disease progression. Am J Ophthalmol. 2016;170:58–67.
46. Zheng F, Zhang Q, Shi Y, et al. Age-dependent changes in the macular choriocapillaris of normal eyes imaged with swept-source optical coherence tomography angiography. Am J Ophthalmol. 2019;200:110–22.
47. Zhang Q, Zheng F, Motulsky EH, et al. A novel strategy for quantifying choriocapillaris flow voids using swept-source OCT angiography. Invest Ophthalmol Vis Sci. 2018;59:203–11.
48. Rinella NT, Zhou H, Zhang Q, et al. Quantifying choriocapillaris flow voids in patients with geographic atrophy using swept-source OCT angiography. Ophthalmic Surg Lasers Imaging Retin. 2019;50:E229–35.
49. Coscas F, Querques G, Forte R, et al. Combined fluorescein angiography and spectral-domain optical coherence tomography imaging of classic choroidal neovascularization secondary to age-related macular degeneration before and after intravitreal ranibizumab injections. Retina. 2012;32:1069–76.
50. Kuehlewein L, Bansal M, Lenis TL, et al. Optical coherence tomography angiography of Type 1 neovascularization in age-related macular degeneration. Am J Ophthalmol. 2015;160:739–48.e2
51. Inoue M, Jung JJ, Balaratnasingam C, et al. A comparison between optical coherence tomography angiography and fluorescein angiography for the imaging of type 1 neovascularization. Investig Ophthalmol Vis Sci. 2016;57:OCT314–23.
52. Veronese C, Maiolo C, Morara M, et al. Optical coherence tomography angiography to assess pigment epithelial detachment. Retina. 2016;36:645–50.
53. Malihi M, Jia Y, Gao SS, et al. Optical coherence tomographic angiography of choroidal neovascularization ill-defined with fluorescein angiography. Br J Ophthalmol. 2017;101:45–50.
54. Tan ACS, Tan GS, Denniston AK, et al. An overview of the clinical applications of optical coherence tomography angiography. Eye. 2018;32(2):262–86.
55. Xu D, Dávila JP, Rahimi M, et al. Long-term progression of Type 1 neovascularization in age-related macular degeneration using optical coherence tomography angiography. Am J Ophthalmol. 2018;187:10–20.
56. Dansingani KK, Tan ACS, Gilani F, et al. Subretinal hyperreflective material imaged with optical coherence tomography angiography. Am J Ophthalmol. 2016;169:235–48.
57. El Ameen A, Cohen SY, Semoun O, et al. Type 2 neovascularization secondary to age-related macular degeneration imaged by optical coherence tomography angiography. Retina. 2015;35:2212–8.
58. Souied EH, Miere A, Cohen SY, et al. Optical coherence tomography angiography of fibrosis in age-related macular degeneration. Dev Ophthalmol. 2016;56:86–90.
59. Cheung CMG, Lai TYY, Ruamviboonsuk P, et al. Polypoidal choroidal vasculopathy: definition, pathogenesis, diagnosis, and management. Ophthalmology. 2018;125:708–24.
60. Kuehlewein L, Dansingani KK, De Carlo TE, et al. Optical coherence tomography angiography of type 3 neovascularization secondary to age-related macular degeneration. Retina. 2015;35:2229–35.
61. Bonini Filho MA, De Carlo TE, Ferrara D, et al. Association of choroidal neovascularization and central serous chorioretinopathy with optical coherence tomography angiography. JAMA Ophthalmol. 2015;133:899–906.
62. de Carlo TE, Romano A, Waheed NK, Duker JS. A review of optical coherence tomography angiography (OCTA). Int J Retin Vitr. 2015;1:5.
63. Coscas GJ, Lupidi M, Coscas F, et al. Optical coherence tomography angiography versus traditional multimodal imaging in assessing the activity of exudative age-related macular degeneration: a new diagnostic challenge. Retina. 2015;35:2219–28.
64. Lumbroso B, Rispoli M, Savastano MC. Longitudinal optical coherence tomography-angiography study of type 2 naive choroidal neovascularization early response after treatment Optical Coherence Tomography View project. Artic Retin. 2015; https://doi.org/10.1097/IAE.0000000000000879.
65. Marques JP, Costa JF, Marques M, et al. Sequential morphological changes in the CNV net after intravitreal anti-VEGF evaluated with OCT angiography. Ophthalmic Res. 2016;55:145–51.
66. Bhutto I, Lutty G. Understanding age-related macular degeneration (AMD): relationships between the photoreceptor/retinal pigment epithelium/Bruch's membrane/choriocapillaris complex. Mol Asp Med. 2012;33:295–317.

67. Dansingani KK, Balaratnasingam C, Klufas MA, et al. Optical coherence tomography angiography of shallow irregular pigment epithelial detachments in pachychoroid spectrum disease. Am J Ophthalmol. 2015;160:1243–54.e2
68. De Carlo TE, Kokame GT, Kaneko KN, et al. Sensitivity and specificity of detecting polypoidal choroidal vasculopathy with en face optical coherence tomography and optical coherence tomography angiography. Retina. 2019;39:1343–52.
69. Tan CS, Hariprasad SM, Lim LW. New paradigms in polypoidal choroidal vasculopathy management: the impact of recent multicenter, randomized clinical trials. Ophthalmic Surg Lasers Imaging Retin. 2018;49:4–10.
70. Tan CS, Lim TH, Hariprasad SM. Current management of polypoidal choroidal vasculopathy. Ophthalmic Surg Lasers Imaging Retin. 2015;46:786–91.
71. Chi Y-T, Yang C-H, Cheng C-K. Optical coherence tomography angiography for assessment of the 3-dimensional structures of polypoidal choroidal vasculopathy. JAMA Ophthalmol. 2017;135:1310–6.
72. Kawamura A, Yuzawa M, Mori R, et al. Indocyanine green angiographic and optical coherence tomographic findings support classification of polypoidal choroidal vasculopathy into two types. Acta Ophthalmol. 2013;91:e474–81.
73. Srour M, Querques G, Semoun O, et al. Optical coherence tomography angiography characteristics of polypoidal choroidal vasculopathy. Br J Ophthalmol. 2016;100:1489–93.
74. Takayama K, Ito Y, Kaneko H, et al. Comparison of indocyanine green angiography and optical coherence tomographic angiography in polypoidal choroidal vasculopathy. Eye. 2017;31:45–52.
75. Tanaka K, Mori R, Kawamura A, et al. Comparison of OCT angiography and indocyanine green angiographic findings with subtypes of polypoidal choroidal vasculopathy. Br J Ophthalmol. 2017;101:51–5.
76. Cheung CMG, Yanagi Y, Akiba M, et al. Improved detection and diagnosis of polypoidal choroidal vasculopathy using a combination of optical coherence tomography and optical coherence tomography angiography. Retina. 2019;39:1655–63.
77. Huang Y-M, Hsieh M-H, Li A-F, Chen S-J. Sensitivity, specificity, and limitations of optical coherence tomography angiography in diagnosis of polypoidal choroidal vasculopathy. J Ophthalmol. 2017;2017:3479695.
78. Choi W, Waheed NK, Moult EM, et al. Ultrahigh speed swept source optical coherence tomography angiography of retinal and choriocapillaris alterations in diabetic patients with and without retinopathy. Retina. 2017;37:11–21.
79. Hwang TS, Jia Y, Gao SS, et al. Optical coherence tomography angiography features of diabetic retinopathy. Retina. 2015;35:2371–6.
80. Ishibazawa A, Nagaoka T, Takahashi A, et al. Optical coherence tomography angiography in diabetic retinopathy: a prospective pilot study. Am J Ophthalmol. 2015;160:35–44.e1
81. Matsunaga DR, Yi JJ, De Koo LO, et al. Optical coherence tomography angiography of diabetic retinopathy in human subjects. Ophthalmic Surg Lasers Imaging Retin. 2015;46:796–805.
82. Parravano M, De Geronimo D, Scarinci F, et al. Diabetic microaneurysms internal reflectivity on spectral-domain optical coherence tomography and optical coherence tomography angiography detection. Am J Ophthalmol. 2017;179:90–6.
83. de Carlo TE, Chin AT, Bonini Filho MA, et al. Detection of microvascular changes in eyes of patients with diabetes but not clinical diabetic retinopathy using optical coherence tomography angiography. Retina. 2015;35:2364–70.
84. Salz DA, De Carlo TE, Adhi M, et al. Select features of diabetic retinopathy on swept-source optical coherence tomographic angiography compared with fluorescein angiography and normal eyes. JAMA Ophthalmol. 2016;134:644–50.
85. Couturier A, Mané V, Bonnin S, et al. Capillary plexus anomalies in diabetic retinopathy on optical coherence tomography angiography. Retina. 2015;35:2384–91.
86. Hwang TS, Miao Z, Bhavsar K, et al. Visualization of 3 distinct retinal plexuses by projection-resolved optical coherence tomography angiography in diabetic retinopathy. JAMA Ophthalmol. 2016;134:1411–9.
87. Agemy SA, Scripsema NK, Shah CM, et al. Retinal vascular perfusion density mapping using optical coherence tomography angiography in normals and diabetic retinopathy patients. Retina. 2015;35:2353–63.
88. Tan CS, Lim LW, Chow VS, et al. Optical coherence tomography angiography evaluation of the parafoveal vasculature and its relationship with ocular factors. Invest Ophthalmol Vis Sci. 2016;57:224–34.
89. Di G, Weihong Y, Xiao Z, et al. A morphological study of the foveal avascular zone in patients with diabetes mellitus using optical coherence tomography angiography. Graefes Arch Clin Exp Ophthalmol. 2016;254:873–9.
90. Freiberg FJ, Pfau M, Wons J, et al. Optical coherence tomography angiography of the foveal avascular zone in diabetic retinopathy. Graefes Arch Clin Exp Ophthalmol. 2016;254:1051–8.
91. Takase N, Nozaki M, Kato A, et al. Enlargement of foveal avascular zone in diabetic eyes evaluated by en face optical coherence tomography angiography. Retina. 2015;35:2377–83.
92. Zhang M, Hwang TS, Dongye C, et al. Automated quantification of nonperfusion in three retinal plexuses using projection-resolved optical coherence tomography angiography in diabetic retinopathy. Invest Ophthalmol Vis Sci. 2016;57:5101–6.
93. Moein HR, Novais EA, Rebhun CB, et al. Optical coherence tomography angiography to detect macular capillary ischemia in patients with inner retinal

changes after resolved diabetic macular edema. Retina. 2018;38:2277–84.
94. Hasegawa N, Nozaki M, Takase N, et al. New insights into microaneurysms in the deep capillary plexus detected by optical coherence tomography angiography in diabetic macular edema. Invest Ophthalmol Vis Sci. 2016;57:OCT348–55.
95. de Carlo TE, Chin AT, Joseph T, et al. Distinguishing diabetic macular edema from capillary nonperfusion using optical coherence tomography angiography. Ophthalmic Surg Lasers Imaging Retina. 2016;47:108–14.
96. Kashani AH, Green KM, Kwon J, et al. Suspended scattering particles in motion: a novel feature of OCT angiography in exudative maculopathies. Ophthalmol Retin. 2018;2:694–702.
97. Lee J, Moon BG, Cho AR, Yoon YH. Optical coherence tomography angiography of DME and its association with anti-VEGF treatment response. Ophthalmology. 2016;123(11) Elsevier Inc.,:2368–75.
98. Kashani AH, Lee SY, Moshfeghi A, et al. Optical coherence tomography angiography of retinal venous occlusion. Retina. 2015;35:2323–31.
99. Rispoli M, Savastano MC, Lumbroso B. Capillary network anomalies in branch retinal vein occlusion on optical coherence tomography angiography. Retina. 2015;35:2332–8.
100. Nobre Cardoso J, Keane PA, Sim DA, et al. Systematic evaluation of optical coherence tomography angiography in retinal vein occlusion. Am J Ophthalmol. 2016;163:93–107.e6
101. Coscas F, Glacet-Bernard A, Miere A, et al. Optical coherence tomography angiography in retinal vein occlusion: evaluation of superficial and deep capillary plexa. Am J Ophthalmol. 2016;161:160–71.e2
102. Sarraf D, Rahimy E, Fawzi AA, et al. Paracentral acute middle maculopathy a new variant of acute macular neuroretinopathy associated with retinal capillary ischemia. JAMA Ophthalmol. 2013;131:1275–87.
103. Rahimy E, Kuehlewein L, Sadda SR, Sarraf D. Paracentral acute middle maculopathy what we knew then and what we know now. Retina. 2015;35:1921–30.
104. Nemiroff J, Kuehlewein L, Rahimy E, et al. Assessing deep retinal capillary ischemia in paracentral acute middle maculopathy by optical coherence tomography angiography. Am J Ophthalmol. 2016;162:121–32.e1
105. Phasukkijwatana N, Rahimi M, Iafe N, Sarraf D. Central retinal vein occlusion and paracentral acute middle maculopathy diagnosed with en face optical coherence tomography. Ophthalmic Surg Lasers Imaging Retin. 2016;47:862–4.
106. Sridhar J, Shahlaee A, Rahimy E, et al. Optical coherence tomography angiography and en face optical coherence tomography features of paracentral acute middle maculopathy. Am J Ophthalmol. 2015;160:1259–68.e2
107. Yu S, Pang CE, Gong Y, et al. The spectrum of superficial and deep capillary ischemia in retinal artery occlusion. Am J Ophthalmol. 2015;159:53–63. e1–2
108. Bakhoum MF, Freund KB, Dolz-Marco R, et al. Paracentral acute middle maculopathy and the ischemic cascade associated with retinal vascular occlusion. Am J Ophthalmol. 2018;195:143–53.
109. McLeod D, Beatty S. Evidence for an enduring ischaemic penumbra following central retinal artery occlusion, with implications for fibrinolytic therapy. Prog Retin Eye Res. 2015;49:82–119.
110. Christenbury JG, Klufas MA, Sauer TC, Sarraf D. OCT angiography of paracentral acute middle maculopathy associated with central retinal artery occlusion and deep capillary ischemia. Ophthalmic Surg Lasers Imaging Retin. 2015;46:579–81.
111. Khan MA, Rahimy E, Shahlaee A, et al. En face optical coherence tomography imaging of deep capillary plexus abnormalities in paracentral acute middle maculopathy. Ophthalmic Surg Lasers Imaging Retin. 2015;46:972–5.
112. Maltsev DS, Kulikov AN, Burnasheva MA, Chhablani J. Prevalence of resolved paracentral acute middle maculopathy lesions in fellow eyes of patients with unilateral retinal vein occlusion. Acta Ophthalmol. 2020;98:e22–8.
113. Bonini Filho MA, Adhi M, de Carlo TE, et al. Optical coherence tomography angiography in retinal artery occlusion. Retina. 2015;35:2339–46.
114. Dingerkus VLS, Munk MR, Brinkmann MP, et al. Optical coherence tomography angiography (OCTA) as a new diagnostic tool in uveitis. J Ophthalmic Inflamm Infect. 2019;9:10.
115. Dutheil C, Korobelnik JF, Delyfer MN, Rougier MB. Optical coherence tomography angiography and choroidal neovascularization in multifocal choroiditis: a descriptive study. Eur J Ophthalmol. 2018;28:614–21.
116. Patel RC, Gao SS, Zhang M, et al. Optical coherence tomography angiography of choroidal neovascularization in four inherited retinal dystrophies. Retina. 2016;36:2339–47.
117. Pichi F, Sarraf D, Arepalli S, et al. The application of optical coherence tomography angiography in uveitis and inflammatory eye diseases. Prog Retin Eye Res. 2017;59:178–201.
118. Türkcü FM, Şahin A, Yüksel H, et al. OCTA Imaging of choroidal neovascular membrane secondary to toxoplasma retinochoroiditis. Ophthalmic Surg Lasers Imaging Retina. 2017;48:509–11.
119. Battaglia Parodi M, Cicinelli MV, Rabiolo A, et al. Vascular abnormalities in patients with Stargardt disease assessed with optical coherence tomography angiography. Br J Ophthalmol. 2017;101:780–5.
120. Arrigo A, Romano F, Aragona E, et al. OCTA-Based identification of different vascular patterns in Stargardt disease. Transl Vis Sci Technol. 2019;8:26.

121. Müller PL, Pfau M, Möller PT, et al. Choroidal flow signal in late-onset stargardt disease and age-related macular degeneration: an OCT-angiography study. Invest Ophthalmol Vis Sci. 2018;59:AMD122–31.
122. Wang JC, Laíns I, Sobrin L, Miller JB. Distinguishing white dot syndromes with patterns of choroidal hypoperfusion on optical coherence tomography angiography. Ophthalmic Surg Lasers Imaging Retina. 2017;48:638–46.
123. Park SS, Thinda S, Kim DY, et al. Phase-variance optical coherence tomographic angiography imaging of choroidal perfusion changes associated with acute posterior multifocal placoid pigment epitheliopathy. JAMA Ophthalmol. 2016;134:943–5.
124. Ong SS, Patel TP, Singh MS. Optical coherence tomography angiography imaging in inherited retinal diseases. J Clin Med. 2019;8:2078.